

Research Report

Surface Labeling with Adhesion Protein FimH Improves Binding of Immunotherapeutic Agent *Salmonella* Ty21a to the Bladder Epithelium

Maroeska J. Burggraaf^{a,1}, Lisette Waanders^{a,1}, Mariska Verlaan^b, Janneke Maaskant^a, Diane Houben^c, Joen Luirink^d, Wilbert Bitter^{a,c}, Coen Kuijl^{a,2} and Carla F.M. Molthoff^{b,2,*}

^aDepartment of Medical Microbiology and Infection Control, Amsterdam University Medical Center (AUMC), Location VU Medical Center (VUMC), Amsterdam, The Netherlands

^bDepartment of Radiology & Nuclear Medicine, Amsterdam University Medical Center (AUMC), Location VU Medical Center (VUMC), Amsterdam, The Netherlands

^cSection Molecular Microbiology, AIMMS, Vrije Universiteit, Amsterdam, The Netherlands

^dAbera bioscience AB, Solna, Sweden

Received 20 August 2020

Accepted 16 November 2020

Pre-press 10 December 2020

Abstract.

BACKGROUND: Bladder cancer is the ninth most common cancer in men. 70% of these tumors are classified as non-muscle invasive bladder cancer and those patients receive 6 intravesical instillations with *Mycobacterium bovis* BCG after transurethral resection. However, 30% of patients show recurrences after treatment and experience severe side effects that often lead to therapy discontinuation. Recently, another vaccine strain, *Salmonella enterica typhi* Ty21a, demonstrated promising antitumor activity *in vivo*. Here we focus on increasing bacterial retention in the bladder in order to reduce the number of instillations required and improve antitumor activity.

OBJECTIVE: To increase the binding of Ty21a to the bladder wall by surface labeling of the bacteria with adhesion protein FimH and to study its effect in a bladder cancer mouse model.

METHODS: Binding of Ty21a with surface-labeled FimH to the bladder wall was analyzed *in vitro* and *in vivo*. The antitumor effect of a single instillation of Ty21a+FimH in treatment was determined in a survival experiment.

RESULTS: FimH-labeled Ty21a showed significant ($p < 0.0001$) improved binding to mouse and human cell lines *in vitro*. Furthermore, FimH labeled bacteria showed ~5x more binding to the bladder than controls *in vivo*. Enhanced binding to the bladder via FimH labeling induced a modest improvement in median but not in overall mice survival.

CONCLUSIONS: FimH labeling of Ty21a significantly improved binding to bladder tumor cells *in vitro* and the bladder wall *in vivo*. The improved binding leads to a modest increase in median survival in a single bladder cancer mouse study.

Keywords: *Salmonella enterica*, Ty21a typhoid vaccine, immunotherapy, bladder cancer, FimH protein, *E. coli*

¹Shared first authors.

²Shared senior authorship.

*Correspondence to: Dr. C.F.M. Molthoff, PhD, associate professor, Department of Radiology & Nuclear Medicine, Amsterdam

University Medical Center (AUMC), location VU University Medical Center (VUMC), Amsterdam, The Netherlands. Tel.: +31 20 444 9291; Fax: +31 20 444 9121; E-mail: cfm.molthoff@amsterdamumc.nl.

ABBREVIATIONS

BCG	<i>Mycobacterium bovis</i> Bacillus Calmette-Guérin
TURB	transurethral resection of the bladder
NMIBC	non-muscle invasive bladder cancer
RD1	region of difference 1
Ty21a	<i>Salmonella enterica typhi</i> Ty21a
UPEC	uropathogenic <i>Escherichia coli</i>
BLI	bioluminescence imaging

INTRODUCTION

Bladder cancer is the ninth most common cancer worldwide and the incidence in men is three times higher than in women [3]. On the other hand, women often show higher stages of cancer at the moment of diagnosis with a concomitant worse prognosis. 70% of the bladder cancers are non-muscle invasive (NMIBC) and are treated by transurethral resection of the bladder (TURB) followed by instillation of the bladder with chemotherapy or immunotherapy to reduce tumor recurrence [4].

Current immunotherapy consists of live *Mycobacterium bovis* Bacillus Calmette-Guérin (BCG), a bacterial vaccine strain well known for its use against tuberculosis in humans. Already since the 1980's BCG is known for its antitumor activity and has been used effectively in bladder cancer treatment [5]. Meta-analysis has shown that treatment with BCG is superior to chemotherapeutic Mitomycin C treatment with less recurrences [6]. However, even from those patients with the best prognosis, still approximately 30% may show recurrence of the tumor or are unable to complete the therapeutic regimen due to severe local and systemic side effects [7].

Recently, *Salmonella enterica typhi* Ty21a (Ty21a) has been shown to exert good potential as antitumor agent in mice [8]. To test the efficacy in humans, a phase I clinical trial has started that investigates Ty21a treatment in NMIBC (Identifier: NCT03421236). Ty21a is an attenuated vaccine strain used against typhoid fever. In an orthotopic bladder cancer mouse model it was shown that already after one instillation, Ty21a could reduce tumor growth and enhance survival, whereas BCG required four treatments to reach equal effects [9]. Furthermore, experiments showing that Ty21a cannot survive in human PBMC cells from

healthy donors, in human cell lines *in vitro* nor in a 3D-bladder tissue *ex vivo* model, suggest a favorable safety profile for Ty21a [8].

To investigate whether Ty21a in bladder cancer therapy can be further optimized, the SpyCatcher/SpyTag system was used. The SpyTag is a short peptide that covalently binds to the SpyCatcher peptide [10]. We use the SpyCatcher/SpyTag technology combined with a modified autotransporter protein that was recently developed by van den Berg van Saparoea [11]. In this system an autotransporter, the hemoglobin protease of *E. coli* (Hbp), lacking the protease activity and carrying a SpyTag, is heterologously expressed in Ty21a cells. This modified Hbp autotransporter is efficiently secreted to the cell surface and allows the covalent attachment of SpyCatcher-labelled proteins to the surface exposed SpyTag peptide sequence [12]. Virtually any target protein that its fused to SpyCatcher can then be efficiently coupled to the SpyTag. This leads to many possibilities for Ty21a treatment optimization while maintaining the Ty21a vaccine safety profile.

We hypothesized that immunotherapeutic efficacy could be improved by enhanced binding of Ty21a to the bladder wall. For BCG immunotherapy binding to the bladder wall has been shown to be important [13] and we hypothesized that the same could hold true for Ty21a treatment. To improve bladder wall binding, the strategy of uropathogenic *E. coli* (UPEC) was used. In this pathogen binding to the bladder epithelium is mediated through Type I pili present on the bacterial cell surface [14]. Type I pili bind host cells through the FimH adhesin at the tip of the pilus. The adhesion domain of FimH binds mannose-sylated proteins on the cell surface of urothelial cells, *e.g.* uroplakin-Ia [1, 2]. FimH is required for binding of UPEC to the bladder wall [15, 16] and thereby important for virulence [17]. We use FimH as an adhesion protein to promote bacterial retention in the bladder.

In this study, we confirm the suitability of the SpyCatcher/SpyTag system to decorate Ty21a with the adhesion domain of FimH. It was shown that the FimH adhesion properties are maintained after coupling to Ty21a *in vitro* with T24, MB49 and Hela cells and *in vivo* with mouse bladders. Furthermore, antitumor activity of Ty21a with and without FimH have been compared in an orthotopic bladder cancer mouse model. The results showed that distinct increased adhesion can be achieved through FimH labeling, but the effect on bladder cancer treatment was limited *in vivo*.

MATERIAL AND METHODS

Mice and tumor cell instillation

C57BL/6 mice (female, 4–6 week old, for intravesical treatment experiments mice obtained from VU University Amsterdam, the Netherlands. For the KRAS and BLI analysis mice were obtained from Charles River, Wilmington, USA) were intravesically instilled with MB49-luc cells as described previously [18]. Briefly, at day 0 mice were anesthetized with 2% isoflurane/oxygen anesthetics (0.4 L/min). Thereafter, mice were catheterized and bladders were rinsed 3 times with PBS. Then the bladder wall was scratched carefully with a 24G blunted needle. Next, 3×10^3 MB49-luc cells were instilled in the bladder and incubated for 2 h. Mice were provided with standard food and water (ad libitum) under conditions described previously. All animal experiments were performed according to the criteria and guidelines of European Community Council Directive 2010/63/EU for laboratory animal care and the Dutch Law on animal experimentation. The experimental protocols (510-RNG19-44; 510-RNG-18-31; 510-RNG19-47A1) were approved by the local committee on animal experimentation of the VU University Amsterdam, The Netherlands (approval number AVD114002016510 / 0510-RNG19-47).

Cells and cell line identity

Murine MB49-luc cells stably expressing luciferase were kindly provided by prof.dr. T. Wurdinger (Amsterdam UMC, location VUmc, Amsterdam, The Netherlands). Cells were cultured in DMEM (Lonza, Verviers, Belgium), supplemented with 10% fetal calf serum (FCS) and 1% penicillin/streptomycin (Gibco Life Technologies, Grand Island, USA). Cells were authenticated by STR analysis (QIAGEN, Hilden, Germany). Luciferase expression was regularly checked by limited dilution methodology for high expressers (BLI, see below).

T24 cells (American Type Culture Collection HTB-4™) were cultured in RPMI1640 with 10% fetal calf serum (FCS; Gibco Life Technologies, Grand Island, USA). HeLa cells were kindly provided by prof. dr. D. Holden (Imperial College London, London, United Kingdom) and were cultured in DMEM with 10% fetal calf serum (FCS; Gibco Life Technologies, Grand Island, USA). RAW264.7 cells (American Type Culture Collection) were cultured in RPMI1640 with Glutamax-1 (Gibco Life

Technologies, Grand Island, USA) supplemented with 10% FCS (Gibco Life Technologies, Grand Island, USA). All cells were cultured at 37°C with 5% CO₂. All cell lines were tested negative for mycoplasma (date last tested: 08/14/2020).

Bioluminescence imaging (BLI)

Mice were anesthetized 2% isoflurane/oxygen anesthetics (0.4 L/min) and abdominal hair was removed. 150 µl D-luciferin (Gold Biotechnology, St. Louis, USA) was subcutaneously injected in the neck region. After 18 minutes, mice BLI signals and X-ray were imaged using the *In-Vivo* Xtreme imager (Bruker, Leiderdorp, the Netherlands) and analyzed by using Bruker Molecular Imaging Software (version 7.5.2.22464).

Bacterial strains

Mycobacterium bovis BCG Tice was cultured in 7H9 liquid medium supplemented with Middlebrook ADC (Difco, BD Biosciences, Franklin Lanes, NJ USA) and 0.05% Tween-80 (Sigma, St. Louis, USA) at 37°C.

S. typhi Ty21a (Mutaflor, Germany) and *E. coli* Top10F' were cultured in LB medium supplemented with 0.2% glucose and, when appropriate, 30 µg/mL chloramphenicol at 37°C and shaking at 200 rpm. For competitive binding experiments LB medium was supplemented with 0.2% glucose and 0.001% galactose. *E. coli* BL-21 were grown in LB supplemented with 50 µM L-rhamnose, 100 µg/ml ampicillin and 30 µg/ml chloramphenicol at 30°C, 200 rpm.

DNA extraction from bladders

Bladders were homogenized with a pestle in TEN buffer (10 mM Tris-HCl, 1 mM EDTA, 100 mM NaCl in aquadest) and incubated overnight at 50°C with 1% SDS and 0.1 mg/ml Proteinase K. DNA was extracted by adding 0.8 volumes phenol/chloroform/isoamyl alcohol (25:24:1), followed by centrifugation. Then, 0.6 volumes isopropanol and NaAc (final conc. 0.3 M) were added to the aqueous phase and incubated for 1 hour at 4°C. After centrifugation, supernatant was removed and the pellet was washed with 70% ethanol. The pellet was dried at RT, dissolved in TE-1 buffer at 65°C for 15 minutes. As control samples, genomic DNA was extracted from RAW and MB49-luc cells in similar fashion.

215 KRAS analysis

216 A fragment spanning the first exon of KRAS was
 217 amplified with primer set KRAS_1_Fw (CTTTA-
 218 CAAGCGCACGCAGAC) and KRAS_1_Rv (AGGT-
 219 TACTCTGTACATCTGTAGTCA) by using Phusion
 220 polymerase (Thermo Scientific, Rockford, USA).
 221 Resulting bands were extracted from a 1% agarose
 222 gel with the GeneJET gel extraction kit (Thermo
 223 Scientific, Rockford, USA) and sent for sequencing
 224 by MacroGen Europe (Amsterdam, the Netherlands)
 225 with primer KRAS_1_Fw or KRAS_1_Rv. Sequence
 226 reads were analyzed by determining the location
 227 of the G>A mutation and use 5 up and down-
 228 stream A and G bases to calculate the average peak
 229 area of these bases on a wild type sequence read.
 230 This average peak area was used to determine the
 231 expected peak area at the mutation site for A and
 232 G. The measured peak area at the location of the
 233 G>A mutation site is divided by either the expected
 234 A or G area, resulting in 2 values for the G>A
 235 mutation: $A \div A(\text{expected}) = \text{mutation frequency}$ and
 236 $1-G \div G(\text{expected}) = \text{mutation frequency}$. The average
 237 of these two values is the fraction of KRAS^{G34A}
 238 positive DNA. Analysis was performed using computing
 239 environment R (R foundation) [19]. Script is
 240 provided in Supplemental Data 1 and 2.

241 Plasmid construction

242 *pET22-pelB-FimH-Spycatcher-his* was created by
 243 inserting the following *pelB-fimH-HA* fragment cod-
 244 ing for the adhesion domain of FimH, amino acids
 245 22–180 in bold, ordered from Integrated DNA Tech-
 246 nologies, Coralville, USA) in *pET22b-spycatcher-his*
 247 vector by In-Fusion cloning (ClonTech, Mountain-
 248 view, USA).

249 ATGAAATACCTGCTGCCGACCGCTGCTGCT
 250 GGTCTGCTGCTCCTCGCTGCCAGCCGGCGA
 251 TGGCCTTTGCATGTAAGACGGCTAATGGCA
 252 CGGCAATTCCAATCGGGGGGGGTAGTGCA
 253 AATGTGTATGTGAATCTTGCGCCCGCTGT
 254 TAATGTGGGACAAAATTTAGTAGTGATT
 255 GTCCACTCAGATTTTCTGTCAATGATTA
 256 TCCAGAACTATCACCGACTATGTGACTCT
 257 GCAACGCGGGGCCGCGTATGGCGGAGTAT
 258 TAAGTCCTTTAGCGGAACGGTAAAATATA
 259 ACGGCTCGTCATACCCATTCCCTACAATT
 260 CTGAGACTCCTCGCGTCGTTTACAATTCC
 261 CGCACTGATAAGCCGTGGCCAGTGGCACT
 262 TTACCTGACCCAGTTTCCAGTGCTGGTG
 263 GAGTTGCTATTAAGCCGGTTCATTGATTG

264 CCGTTTTGATTTTACGCCAAACAACAACACT
 265 ATAACAGTGACGACTTCCAATTCGTGTGGA
 266 ACATCTATGCCAACAACGATGTTGTGGTCC
 267 CAACAGGCAGCGGCGGATATCCCTACGATGT
 268 ACCGGATTACGCTGGATCCGGGGGTACCGGC.

269 *mScarlet* was amplified from template plasmid
 270 *pET11A-mScarlet* (Abera Bioscience, Stockholm,
 271 Sweden) with primers *pEH3-Scarlet-Fw* (GAACAC
 272 ATCTCTGGATCGAACTTTAAGAAGGAGATATA
 273 CATAATGGTGAGCAAG) and *pEH3-Scarlet-Rv*
 274 (GTAAAACGACGGCCAGTGCTACTTGTACAG
 275 CTCGTCCATGC) by phusion polymerase (Thermo
 276 Scientific, Rockford, USA). *neonGreen* was ampli-
 277 fied from *pet22b-Neongreen-SpC-His* (Abera Bio-
 278 science, Stockholm, Sweden) with primers *Hbp-NG-
 279 Fw* (GAACACATCTCTGGATCGAAGAAGGAGA
 280 TATACATATGGTAAGTAAAAG) and *Hbp-NG-Rv*
 281 (GTAAAACGACGGCCAGTGCTACCTTGTACA
 282 GCTCGTCCATGC). The resulting amplicons were
 283 inserted in *pEH3-HbpD(d1)SpyTag* (Abera Bio-
 284 science, Stockholm, Sweden) by restriction with
 285 *EcoRI* (NEB, Ipswich, USA) followed by Gibson
 286 assembly, creating vectors *pEH3-HbpD(d1)SpyTag-
 287 mScarlet* and *pEH3-HbpD(d1)SpyTag-neonGreen*.
 288 Both vectors harbor the *SpyTag* at the N-terminus of
 289 *Hbp*.

290 *E. coli* BL-21 were transformed with *pET22b-
 291 pelB-FimH-spycatcher-his* by standard heat-shock
 292 protocol.

293 *S. typhi* Ty21a were washed with 10% glycerol
 294 and electroporated with *pEH3-HbpD(d1)SpyTag-
 295 mScarlet* and *pEH3-HbpD(d1)SpyTag-neonGreen*.

296 Isolation FimH-SpyCatcher

297 FimH-SpyCatcher was isolated from the periplas-
 298 mic fraction of *E. coli* BL-21 expressing *pET22b-
 299 pelB-FimH-spycatcher-his*. At OD₆₀₀ = 0.3, bacteria
 300 were incubated for 2 hours with 400 μM isopropyl
 301 β-D-1-thiogalactopyranoside (IPTG) to induce exp-
 302 ression. Bacteria were harvested and washed with
 303 20 mM tris(hydroxymethyl)aminomethaan (Tris)
 304 (pH 8). Pellets were resuspended in 20 mM Tris
 305 (pH 8) with 2 mg/ml lysozyme and proteinase
 306 inhibitor mix (Roche). Sphaeroplast formation
 307 was stabilized by adding 10 mM MgCl₂ at a con-
 308 version of 90%. Sphaeroplasts were removed by
 309 centrifugation and the soluble FimH-SpyCatcher
 310 containing supernatant was dialyzed to remove
 311 EDTA. FimH-SpyCatcher was subsequently isolated
 312 by His-purification according to manufacturer's pro-
 313 tocol (TALON Superflow, GE Healthcare, Chicago,

314 USA). The eluate was dialyzed to remove imidazole
315 and the concentration was determined by a BCA
316 assay according to manufacturer's protocol (Thermo
317 Scientific, Rockford, USA).

318 *FimH labeling*

319 Labeling was performed using the SpyTag-Spy
320 Catcher system [12, 20]. Hemoglobin protease (Hbp)
321 was used as a carrier to enable surface exposure of the
322 SpyTag [21]. Overnight pre-culture of bacteria was
323 diluted to $OD_{600}=0.05$ and grown to $OD_{600}=0.3$
324 when Hbp-SpyTag expression was induced with 1
325 mM IPTG and incubated for 3h at 37°C. To prevent
326 binding of excessive unbound FimH to unlabeled bac-
327 teria in competition experiments, non-labeled Ty21a
328 bacteria were labeled with recombinant SpyCatcher-
329 maltose binding protein (MPB). Then, bacteria were
330 harvested and washed with PBS. Bacteria were
331 resuspended in PBS and incubated with 40 μ g FimH-
332 HA-SpyCatcher overnight at 4°C. Bacteria were
333 washed once with PBS before use and resuspended
334 in Krebs-Ringer-HEPES buffer (KRP) supplemented
335 with 1.85 mM calcium and 1.3 mM Mg.

336 *Binding assays*

337 MB49-luc (160.000 cells/well), T24 (160.000
338 cells/well) and HeLa (60.000 cells/well) were incu-
339 bated with an equivalent of $OD_{600}=0.05$ FimH
340 labeled or unlabeled bacteria for 1 h and then washed
341 with KRP with 1.85 mM calcium and 1.3 mM Mg.
342 Cells were fixated with 4% PFA (Sigma, St. Louis,
343 USA) for 30 minutes. HeLa cells were permeabi-
344 lized with 0.1% Triton-X100 (Sigma, St. Louis, USA)
345 and incubated 15 minutes on ice. After washing with
346 PBS, cells were stained with Hoechst (1:2000 in PBS,
347 Invitrogen, Carlsbad, USA) and Oregon Green™
348 488 Phalloidin (1:200 in PBS, Invitrogen, Carlsbad,
349 USA).

350 For competitive binding assays, FimH labeled and
351 MBP labeled bacteria were mixed in a 1:1 ratio in
352 PBS with 1 mM calcium and 1 mM Mg. Bacteria were
353 washed with and diluted in PBS. Mice were intravesi-
354 cally instilled with 100 μ l bacterial mix (17.4×10^5
355 CFU) for 1 hour according to the procedure for intrav-
356 esical instillation described above. After sacrificing
357 the mice, bladders were fixated with 4% PFA for 1.5
358 hours and resected from the mice. Bladders were cut
359 open, 3 times washed with PBS and incubated in
360 Hoechst (1:500 in PBS, Invitrogen, Carlsbad, USA)
361 for 1 hour. Then, bladders were put under a coverslip

with Vectashield antifade mounting medium (H-
1000, Vector Laboratories, Peterborough, UK) and
sealed with cover sealant (Biotium, Fremont, USA).

365 *Microscopical analysis*

366 Widefield microscopic images of *in vitro* exper-
367 iments were taken with Olympus IX83 inverted
368 microscope analyzed with cell image analysis soft-
369 ware (Cellprofiler version 3.1.5). The fluorescent
370 intensities of Ty21a mScarlet signal were determined
371 when associated with GFP-actin defined HeLa cells.
372 The mScarlet signals (Z) depicted in the graphs are
373 normalized by the formula $Z=(x-\min)/(\max-\min)$, in
374 which x is the raw mScarlet signal, min is the low-
375 est mScarlet signal and max is the highest mScarlet
376 signal. Ratios of labeled/unlabeled bacteria were cor-
377 rected for the input ratios.

378 Whole mounted bladders of the *in vivo* competi-
379 tive binding experiment were imaged with confocal
380 microscopy (Nikon A1 plus). Pixels that showed a
381 fluorescent signal of mScarlet or NeonGreen were
382 counted in each Z-stack of every image. Pixel counts
383 were accumulated for all images per mouse and cor-
384 rected for the input CFU (as counted by CFU plating).
385 Then, the ratio NeonGreen/mScarlet pixels per mouse
386 was calculated.

387 *Immunoblot analysis*

388 Bacteria were washed with PBS and resuspended
389 in SDS sample buffer (50 mM Tris-HCl, 100
390 mM dithiothreitol (DTT), 2% sodium dodecyl sul-
391 phate (SDS), 5 mM ethylenediaminetetraacetic acid
392 (EDTA), 10% glycerol). Samples were separated by
393 SDS PAGE and transferred to a nitrocellulose filter
394 by Western blotting. Blots were blocked with 5%
395 milk in PBS and stained with anti-HA (HA 1.11)
396 and goat-anti-mouse IgG peroxidase-labelled anti-
397 bodies (American Qualex Antibodies, San Clemente,
398 USA). Imaging was performed with electro-chemi-
399 luminescence Western Blotting Detection Reagent
400 (Amersham Bioscience, Amersham, UK).

401 *Survival experiment*

402 Mice were anesthetized and catheterized and
403 instilled with MB49-luc on day 0 as described above
404 and after rinsing bladders, mice were instilled with
405 100 μ l Ty21a coupled to FimH, Ty21a or PBS on
406 day 5, aiming for 3×10^7 CFU Ty21a (actual CFU
407 without FimH: 3.7×10^7 , with FimH: 2.4×10^7)

408 and incubated for 1h. Input CFU was determined
409 based on study by Domingos-Pereira *et al.* 2016
410 [8]. BLI was measured at day 8, only mice that
411 showed positive BLI signal (at least 1.5x higher intensi-
412 ty than the background signal) continued in the
413 experiment. Bodyweight was monitored 3 times per
414 week and overall well-being was evaluated every day.
415 Sacrificed mice that did not show a bladder tumor
416 upon resection were not included in Kaplan-Meier
417 analysis.

418 *Statistical analysis*

419 Ty21a binding with or without FimH *in vitro* was
420 analyzed with an unpaired T test. Fold change binding
421 in competition experiment with FimH labeled bacte-
422 ria was analyzed with a one-sample *t*-test. The median
423 survival was analyzed by Wilcoxon-signed rank test.

424 **RESULTS**

425 *Labeling of Ty21a with FimH to improve bladder* 426 *binding*

427 We hypothesized that *S. enterica typhi* Ty21a
428 immunotherapy can be improved by enhancing
429 adhesion of the bacteria to the bladder wall, as
430 adhesion is the first important and essential step in
431 BCG immunotherapy [13]. To examine this, bacteria
432 were labelled with FimH by using Hbp autotrans-
433 porter SpyCatcher/SpyTag system [11]. Using this
434 method, the FimH protein is not expressed con-
435 stitutively, but the bacterial cell surface is only
436 decorated extensively with the adhesion domain of
437 FimH before installation. In the system described
438 by van den Berg van Saparoea the Hbp protein
439 is abundantly expressed on the bacterial cell sur-
440 face and modified to expose a spytag at the distal
441 end [11]. Subsequently, these bacteria are incu-
442 bated with recombinant SpyCatcher-FimH carrying
443 an HA-tag. The binding of SpyCatcher to SpyTag
444 results in a spontaneous intramolecular isopeptide
445 bond and thus the covalent attachment of FimH to
446 the surface of Ty21a. The formation of the FimH-
447 Spycatcher:Hbp-SpyTag complex was analyzed by
448 immunoblot analysis using HA antibodies (Fig. 1A).
449 Upon incubation with the SpyCatcher-HA-FimH pro-
450 tein the appearance of a protein conjugate with the
451 predicted molecular weight of ~140kDa could be
452 observed, indicating that the conjugation was suc-
453 cessful (Fig. 1A).

To determine whether FimH could improve bind- 454
ing *in vitro*, FimH-labeled Ty21a bacteria were 455
incubated with the human epithelial cell line HeLa. 456
FimH-labeled Ty21a showed significantly more bind- 457
ing to HeLa cells as compared to unlabeled bacteria 458
($p < 0.0001$) (Fig. 1B). Subsequently, we tested the 459
binding of FimH-labeled Ty21a bacteria to a human 460
and a murine bladder cancer cell line, T24 and MB49, 461
respectively. Again, a highly improved binding was 462
observed (Fig. 1B), indicating that the binding char- 463
acteristics of Ty21a have been significantly improved 464
by FimH surface labeling. 465

Next, the effect of FimH labeling on binding of 466
bacteria to the bladder wall was studied *in vivo* in 467
C57BL/6 mice. In a competition assay, bladders were 468
instilled with a mixture of FimH labeled (expressing 469
NeonGreen) and MBP labeled (expressing mScarlet) 470
Ty21a bacteria. MBP was used to prevent binding 471
of excess FimH to the mScarlet Ty21a control by 472
binding to the SpyTag present in Hbp. Microscop- 473
ical analysis showed that bacteria were not evenly 474
distributed over the tissue, but appeared in patches 475
(Fig. 1C). A minimum of 4 of these patches per 476
mouse ($n = 7$) were analyzed for binding of FimH 477
labeled and unlabeled bacteria by fluorescent con- 478
focal microscopy (Fig. 1C). FimH-labeled bacteria 479
showed 4.9 times more binding than unlabeled bac- 480
teria ($p = 0.005$). This is in agreement with the *in* 481
vitro obtained results. These experiments showed an 482
improved binding of *S. enterica typhi* Ty21a bacteria 483
to the bladder wall upon decoration with the adhesion 484
domain FimH. 485

486 *Read-out analysis of tumor growth*

To investigate the effect of Ty21a coupled to FimH 487
in a bladder cancer mouse model, a reliable method 488
is needed to determine tumor take and preferably 489
tumor size as well. Tumor growth can be measured 490
in vivo by bioluminescence imaging (BLI) and *ex* 491
in vivo by assessing bladder weight. However, although 492
monitoring tumor growth over time *in vivo* can be 493
instrumental, it is not clear yet whether BLI can be 494
used as an exact measure of tumor growth. Bladder 495
weight on the other hand might be affected by influx 496
of healthy stromal cells and immune cells into the 497
tumor. To determine which method is most reliable 498
to measure tumor growth, we compared BLI signals, 499
tumor weight and DNA compositions of untreated 500
bladders at several days after tumor cell installation. 501
For this, 15 mice were instilled with MB49 tumor 502

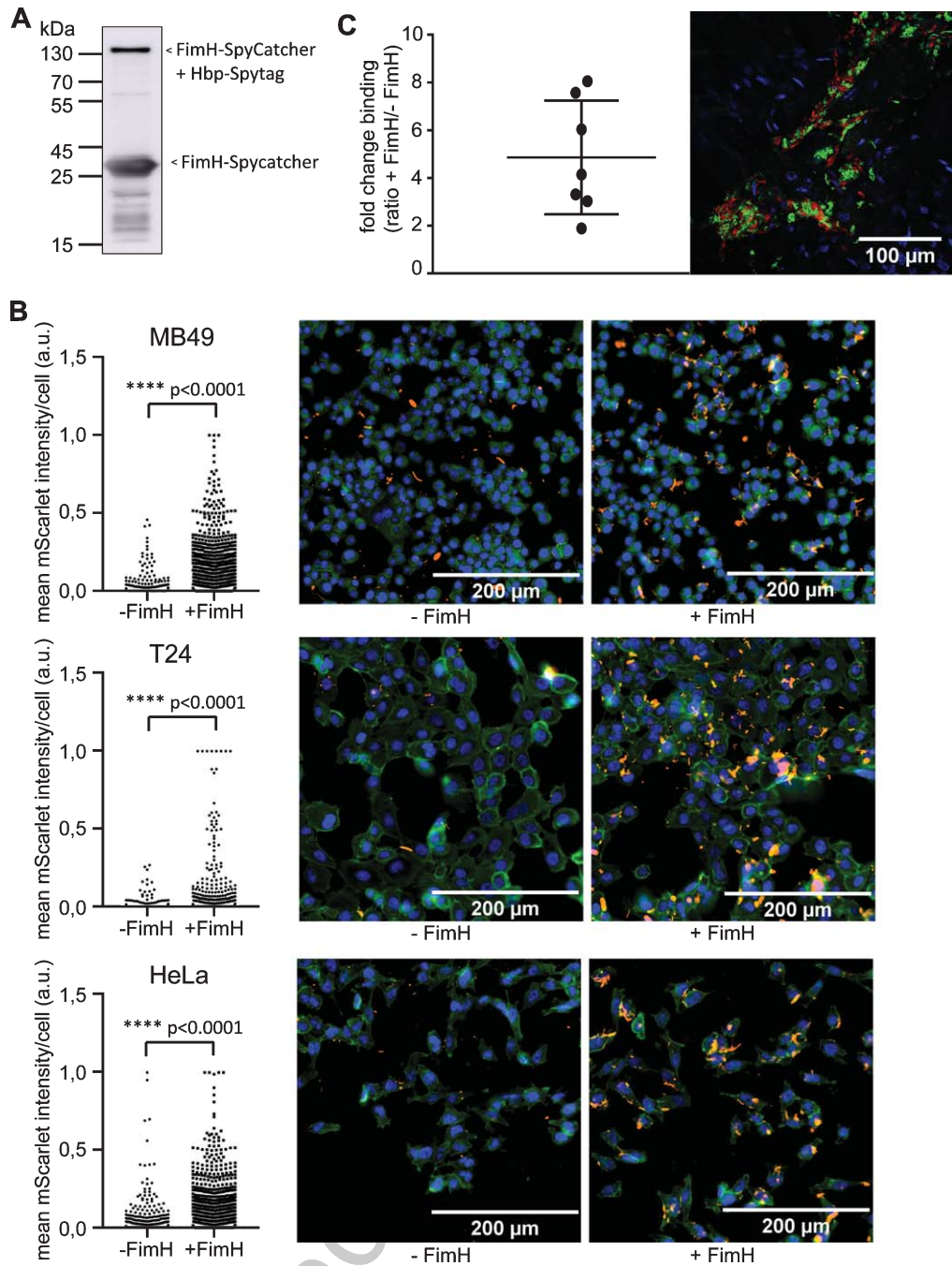


Fig. 1. Analysis of bacterial binding upon surface labeling of *S. enterica typhi* Ty21a with FimH. (A) Immunoblot showing FimH-SpyCatcher (~30 kDa) and Hbp-SpyTag labeled with FimH-HA-SpyCatcher (~140 kDa) as present in labeled Ty21a. Bacterial pellet representing 0.1 OD units (OD_{600}) was loaded and polyclonal antiserum directed against the HA tag was used. (B) Fluorescent microscopy images of MB49, T24 and HeLa cells incubated for 1 h with FimH labeled (+FimH) or unlabeled (-FimH) Ty21a (red). After fixation, actin was stained in green and nuclei in blue. Graph shows mean mScarlet intensity/cell for unlabeled Ty21a (-FimH) and FimH labeled Ty21a (+FimH). Intensities were corrected for input CFU. Statistical analysis: unpaired *T*-test. (C) Mice were instilled with a mix of FimH labeled Ty21a (neonGreen) and MBP labeled Ty21a (mScarlet). Confocal microscopy z-stack images of a minimum of 3 patches per mouse ($n = 7$) were scored for the presence of neonGreen and mScarlet bacteria. Representative single slide of z-stack is shown. Fold change binding depicts the ratio of neonGreen/mScarlet bacteria after correction for input CFU. Statistical analysis: one sample *T*-test.

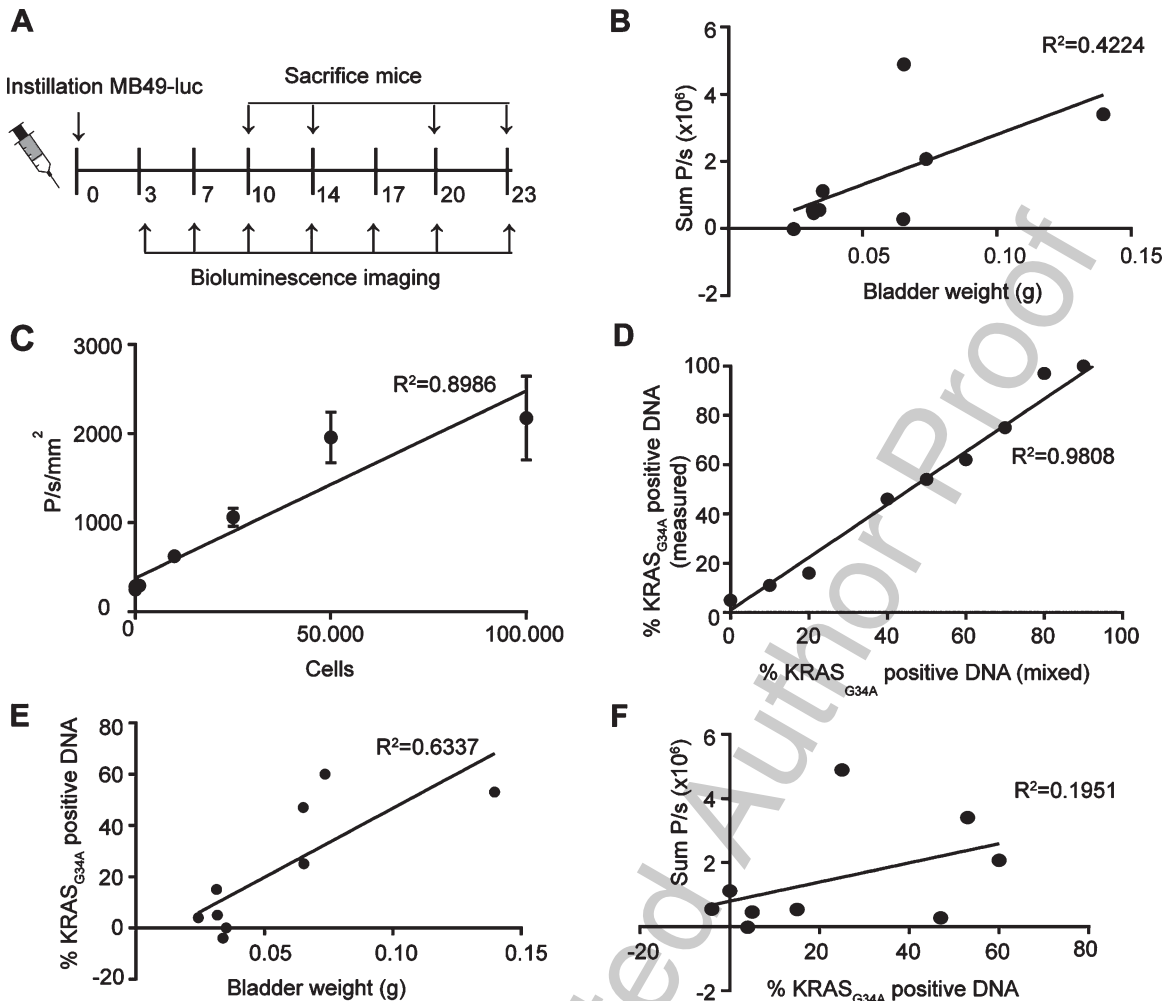


Fig. 2. Comparison BLI and bladder weight for analysis of tumor growth. (A) Schematic overview of experimental set-up. (B) Correlation plot of BLI signal over bladder weight ($n=9$). (C) *In vitro* analysis of BLI signal of MB49-luc cells. (D) Correlation plot of KRAS_{G34A} positive DNA as measured by sequencing over KRAS_{G34A} positive DNA as mixed before sequencing. Genomic DNA was isolated from RAW cells (KRAS_{G34}) and MB49-luc (KRAS_{A34}) and mixed in depicted proportions. (E) Correlation plot of percentage of KRAS_{G34A} positive cells as determined by sequence analysis over bladder weight ($n=9$). (F) Correlation plot of BLI signal and percentage of KRAS_{G34A} positive DNA ($n=9$). (B,E,F) Only bladders with tumors were taken into account.

503 cells expressing luciferase, and BLI was measured
 504 at day 3, 7, 10, 14, 17, 20 and 23 after instillation.
 505 To compare different tumor sizes with BLI measure-
 506 ments, 3–5 mice were sacrificed at days 10, 14, 20
 507 and 23 and bladders were isolated for further analysis
 508 (Fig. 2A).

509 After tumor cell instillation 9 out of 15 mice
 510 had developed a tumor at the day of sacrifice as
 511 based on macroscopic analysis. Only bladders with
 512 a tumor were taken into account for further analysis.
 513 Tumor-bearing bladders did not show a significant
 514 correlation between the BLI signal and the blad-
 515 der weight ($R^2=0.4224$, $p=0.0581$)(Fig. 2B, see

Supplemental Data 3 for all bladders). This might
 516 seem remarkable, since BLI signal shows a linear
 517 relationship with the number of MB49-luc cells *in*
 518 *vitro* ($R^2=0.8986$, $p=0.0003$) (Fig. 2C). Although
 519 the low amount of tumor bearing bladders make it
 520 difficult to find a significant correlation, the low
 521 correlation might also be due to the contribution of
 522 non-tumor cells to the total tumor weight *in vivo*.
 523

To determine the percentage of MB49 cells from
 524 the total amount of cells in the tumor, we analyzed
 525 the DNA of the bladders with tumors for the pres-
 526 ence of a specific mutation in KRAS. This mutation
 527 is present in MB49-luc cells but not in wild type
 528

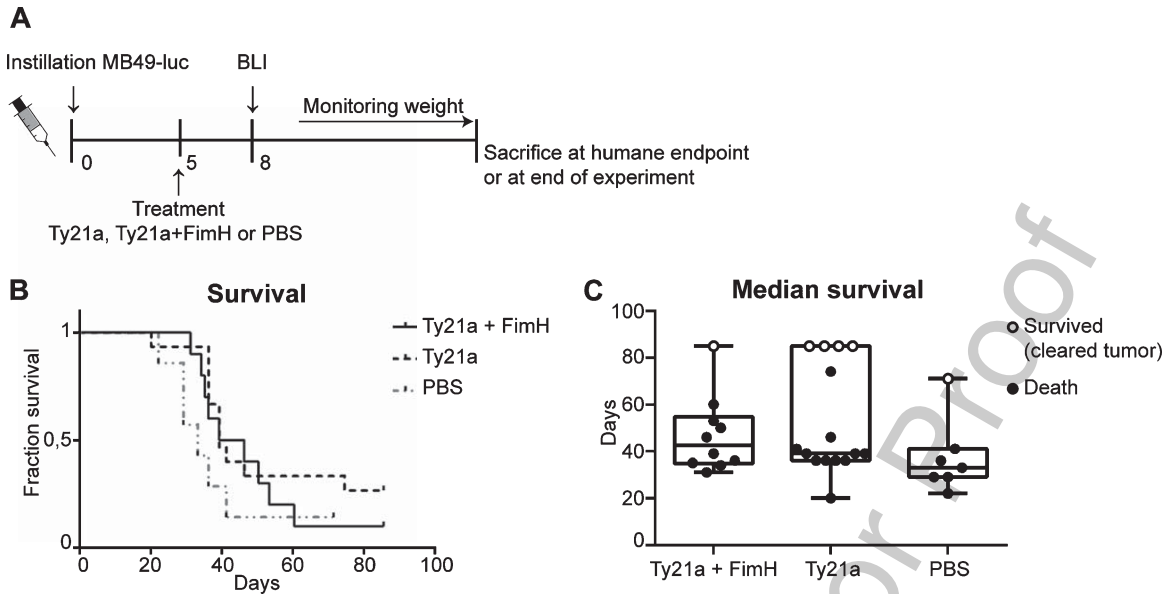


Fig. 3. Survival experiment bladder cancer mouse model with Ty21a and FimH treatment. (A) Schematic overview of experimental set-up. Mice received 3×10^3 MB49-luc cells at day 0 and were treated at day 5. Mice that developed tumors at day 8 according to BLI Ty21a+FimH ($n=10$), Ty21a ($n=15$) and PBS ($n=7$) were included for survival analysis. (B) Kaplan-Meier curve showing survival of mice treated with Ty21a+FimH, Ty21a and PBS. (C) Median survival of different treatment groups. Mice which died and showed a bladder tumor upon macroscopic analysis are presented as filled circles. Mice which showed no sign of a bladder tumor upon macroscopic analysis are considered 'cured'. These are presented as open circles.

529 cells of C57BL/6 mice [22]. Control samples with
530 a known percentage of MB49-luc DNA showed a
531 linear relationship between the percentage of DNA
532 with the KRAS_{G34A} mutation and the percentage of
533 DNA with or without the KRAS_{G34A}, as calculated
534 from the relative peak area for the mutated base in
535 the sanger sequence trace ($R^2 = 0.9808$, $p < 0.0001$)
536 (Fig. 2D).

537 Genomic DNA of the bladders was isolated and
538 the percentage of KRAS_{G34A} positive DNA present
539 was determined. A significant correlation was found
540 between bladder weight and the percentage of
541 KRAS_{G34A} positive DNA ($R^2 = 0.6337$, $p = 0.0103$)
542 (Fig. 2E). In contrast, no correlation was found for
543 the percentage of KRAS_{G34A} positive DNA with the
544 BLI signal ($R^2 = 0.1951$, $p = 0.2339$) (Fig. 2F), sug-
545 gesting that the BLI signal is not an accurate measure
546 of tumor size.

547 In conclusion, bladder weight is a reliable measure
548 for the amount of tumor cells and thus to measure anti-
549 tumor activity but not feasible in a longitudinal study
550 since bladder weight can only be assessed *ex vivo*. In
551 contrast, BLI is less reliable but can give an indica-
552 tion of tumor take and initial tumor growth *in vivo*.
553 For our following *in vivo* experiment, we therefore
resorted to BLI to solely assess tumor take.

Survival experiment using Ty21a labeled with FimH

554 *S. enterica typhi* Ty21a coupled to FimH showed
555 significant improved binding *in vitro* and *in vivo*.
556 We continued this research by investigating whether
557 improved binding would also improve bladder cancer
558 therapy. Therefore, a well-designed single mice
559 survival experiment with the orthotopic bladder cancer
560 mouse model was conducted. Mice were treated 5
561 days after tumor instillation with either Ty21a+FimH,
562 Ty21a or PBS (Fig. 3A). At day 8 after instillation
563 tumor take was verified with BLI to determine which
564 mice were to be included in the *in vivo* study. Day
565 8 was chosen based on previous experiments showing
566 tumor growth from day 7 [18]. Overall survival
567 curves did not show a significant effect of Ty21a,
568 either coupled to FimH or not, as compared to the
569 PBS treated control mice (Fig. 3B). The highest
570 median survival is seen in the TY21a+FimH treated
571 group (42,5 days), followed by Ty21a (39 days)
572 and PBS (33 days) (Fig. 3C). These results indicate
573 that, although *S. enterica typhi* Ty21a cells do have
574 a modest positive effect on the median survival in
575 the bladder cancer mouse model, this effect is not
576 improved upon enhanced bladder wall attachment
577 (Ty21a+FimH:Ty21a $p = 0.2031$).

DISCUSSION

Resection of the tumor followed by intravesical BCG immunotherapy is the current standard treatment for non-muscle invasive bladder cancer in human. However, even with BCG therapy still ~30% recurrences occur [7, 23]. Furthermore, about 65% of patients report local or systemic side effects with BCG treatment. In 8% of these cases, treatment was discontinued and only 16% of the patients received all scheduled maintenance therapies [24, 25]. The majority of patients did not adhere to the 3 year treatment and did therefore not receive all scheduled instillations [24, 26]. Therefore, improving intravesical bladder cancer therapy is necessary.

In a previous study, it was shown that *S. enterica typhi* Ty21a is significantly better as compared to BCG in the treatment regimen in bladder cancer in mice [8, 9]. Currently, a phase I clinical trial has started with Ty21a in NMIBC (NCT03421236). The classical effective treatment regimen to study BCG immunotherapy in orthotopic bladder cancer mouse models consists of 4 treatments at one week intervals, starting 1 day after tumor instillation. Interestingly, it was shown that Ty21a required only one instillation, whereas BCG requires 4 instillations to induce partial antitumor activity [8]. With the single instillation in case of Ty21a several advantages can be envisioned, such as to greatly reduce the number of anesthetizing and catheterization rounds. If the latter also holds true for the clinical situation, it would also greatly reduce the discomfort for patients which often leads to discontinued treatment. Therefore, in this study we tested whether Ty21a treatment could be further improved by increasing the binding of Ty21a to the bladder epithelium by decorating the bacteria with adhesion protein FimH.

An important advantage of Ty21a compared to BCG is its safety profile. Ty21a is an attenuated strain of *S. enterica typhi* not able to survive within cells, but harboring the capacity to evoke immune responses [9, 27]. Another advantage of Ty21a is the lack of disseminating capacity to other organs like spleen and lymph nodes in the mouse after intravesical instillation. Furthermore, Ty21a does not survive in human cells nor in an 3D-bladder-tissue ex vivo assay, suggesting an improved safety profile as compared to BCG [8].

With respect to cystitis, the main adverse local side-effect of BCG therapy in approximately 35% of clinical cases [24], it was reported that *E. coli* FimH enhances the ability to traffic from the bladder to

deeper tissues and initiate cystitis [28]. Theoretically, labeling Ty21a with FimH could therefore enable dissemination. To prevent conceivable dissemination of FimH-labeled-Ty21a, Ty21a was not recombinantly modified to express type I pili. In our approach we labeled extracellularly with purified adhesion domain of FimH via the SpyCatcher/SpyTag system. This means that the pilus is not intact. Furthermore, FimH is not genetically encoded in Ty21a, hence daughter cells will not harbor FimH on their cell surface and the possibility of dissemination facilitated through FimH will be restricted.

First, the study aimed to improve binding of Ty21a to the bladder epithelium by decorating Ty21a with FimH. FimH has been shown before to be crucial for binding to the urothelium in *E. coli* [28]. Here we showed that labeling Ty21a with FimH increased binding to bladder cancer cell lines T24 and MB49 but also epithelial cell line HeLa. Moreover, competition experiments with FimH labeled and MBP labeled Ty21a showed 4.8 times more binding to the bladder for FimH labeled bacteria. Importantly, the FimH adhesion domain was able to increase binding not only when part of the type I pili complex in *E. coli*, but also when linked to the cell surface protein Hbp on Ty21a.

We also assessed the accuracy of BLI for measuring tumor growth *in vivo*. A previous study demonstrated that BLI signals reach a plateau over time while tumor size increases, as was confirmed by high resolution ultrasound imaging [18]. Here, we looked in more detail to the correlations between BLI and bladder weight. Analysis of the tumor composition, *e.g.* the percentage of MB49-luc tumor cells present, showed that the percentage of tumor DNA correlated with the bladder weight. This indicates that, as expected, MB49-luc cells are the main cell type present in the tumor. However, no significant correlation was found for the BLI signal and the bladder weight. Thus, bladder weight is a more accurate measure of tumor growth than BLI, but can obviously not be assessed *in vivo*.

The discrepancy between BLI signal and tumor size can be explained by several factors. First, the chemical reaction of luciferase with luciferin requires oxygen and ATP. By photoacoustic imaging it was shown that the amount of oxygen available in the bladder tumor decreases over time [18]. Secondly, the BLI signal might be hindered by light-scattering in deep-tissue. Hence, BLI is very useful for easy tumor growth measurement during the initial period after tumor cell instillation, but other image modalities,

681 such as high resolution ultrasound, preferably com- 730
 682 bined with photoacoustic imaging, would be more 731
 683 representative to determine precise tumor volumes 732
 684 as well as the oxygenation of the tissue. However, 733
 685 photoacoustic imaging is not widespread available as 734
 686 compared to BLI measurement. For orthotopic tumor 735
 687 models in general an advice would be to use BLI to 736
 688 determine tumor presence in combination with high 737
 689 resolution ultrasound and photoacoustic imaging to 738
 690 evaluate *in vivo* tumor behavior. 739

691 The goal of coupling FimH to Ty21a is to have 740
 692 a safe and immunogenic regimen which reduces the 741
 693 number of instillations required for successful treat- 742
 694 ment. The orthotopic bladder cancer model is a good 743
 695 model for determining the effect of coupled FimH 744
 696 to Ty21a in NMIBC disease. Our hypothesis was 745
 697 that improved adhesion to the bladder generates a 746
 698 strong antitumor response, as a consequence of pro- 747
 699 longed exposure of the the immune system to the 748
 700 pathogen. Despite a significant improved binding of 749
 701 Ty21a+FimH to the bladder wall, a strong additional 750
 702 effect of FimH on mouse survival was not observed 751
 703 in a single *in vivo* study. Only a modest improvement 752
 704 in the median survival of Ty21a+FimH (42,5 days) 753
 705 compared to Ty21a alone (39 days) was revealed. 754
 706 However, improvement of therapy probably requires 755
 707 more than enhanced binding to the bladder wall. 756
 708 The Hbp platform with SpyCatcher/SpyTag system 757
 709 allows in addition to FimH, also the coupling of other 758
 710 proteins that can elicit a desired immune response. 759

711 In conclusion, coupling FimH with the Spy- 760
 712 Catcher/SpyTag technology provides an efficient 761
 713 method to decorate Ty21a. Importantly, coupling 762
 714 does not interfere with protein function of FimH or 763
 715 antitumor activity of Ty21a. This method is therefore 764
 716 a promising strategy to optimize antitumor directed 765
 717 responses. The enhanced bacterial binding did not 766
 718 result in significantly better bladder cancer survival 767
 719 *in vivo*, unfortunately. Nevertheless, it would be 768
 720 interesting to analyze the immune responses more 769
 721 extensively to have a better understanding of which 770
 722 responses are required for antitumor activity. The 771
 723 combination of prolonged exposure of the bladder to 772
 724 Ty21a with coupled FimH and/or immunoregulatory 773
 725 target proteins might be the key for the improvement 774
 726 of bladder cancer therapy. 775

727 ACKNOWLEDGMENTS

728 Expert technical help of Bart van den Berg van 776
 729 Saproea is greatly acknowledged. Also, we thank 777

Peter van Ulsen for lively discussions and provid- 730
 ing the recombinant FimH-SpyCatcher, which was 731
 isolated by Tamara Hillenaar and Lea Adolf. 732

733 FUNDING

This work was supported by funding of the Cancer 734
 Center Amsterdam ('VUmc CCA Huijgens Program' 735
 to MJB). 736

737 AUTHOR CONTRIBUTIONS

Conception: MJB, LW, JL, WB, CK, CFM 738
 Performance of work: MJB, LW, MV, JM, DH 739
 Interpretation or analysis of data: MJB, LW, CK 740
 Writing the article: LW, MJB, CFM, WB, CK 741

742 CONFLICT OF INTEREST

Maroeska J. Burggraaf, Lisette Waanders, Mariska 743
 Verlaan, Janneke Maaskant, Diane Houben, Joen 744
 Luirink, Wilbert Bitter, Coen Kuijl and Carla F.M. 745
 Molthoff have no conflict of interest to report. 746

747 SUPPLEMENTARY MATERIAL

Script for K-Ras analysis (Data 1 and 2) 748
 BLI and bladder weight of all mice included in 749
 read-out experiment (Data 3) 750
 The supplementary material is available in the 751
 electronic version of this article: [https://dx.doi.org/](https://dx.doi.org/10.3233/BLC-200382) 752
[10.3233/BLC-200382](https://dx.doi.org/10.3233/BLC-200382). 753

754 REFERENCES

- 755 [1] Wu X, Sun T, Medina JJ. In vitro binding of type 1- 756
 757 fimbriated *Escherichia coli* to uroplakins Ia and Ib: Relation 758
 to urinary tract infections. *Proc Natl Acad Sci U S A*. 1996; 759
 93:9630-35. 760
- 761 [2] Xie B, Zhou G, Chan SY, Shapiro E, Kong XP, Wu XR, 762
 Sun TT, Costello CE. Distinct glycan structures of uro- 763
 plakins Ia and Ib: structural basis for the selective binding of 764
 FimH adhesin to uroplakin Ia. *J Biol Chem*. 2006;281(21): 765
 14644-53. 766
- 767 [3] Berdik C. Unlocking bladder cancer. *Nature*. 2017;551: 768
 S34-35. 769
- 770 [4] Babjuk M, Bohle A, Burger M, Capoun O, Cohen D, Com- 771
 perat EM, Hernandez V, Kaasinen E, Palou J, Roupert 772
 M, van Rhijn BW, Shariat SF, Soukup V, Sylvester RJ, 773
 Zigeuner R. EAU Guidelines on Non-Muscle-invasive 774
 Urothelial Carcinoma of the Bladder: Update 2016. *Eur 775
 Urol*. 2016;71(3):447-61. 776
- 777 [5] Pettenati C, Ingersoll MA. Mechanisms of BCG 778
 immunotherapy and its outlook for bladder cancer. *Nat Rev 779
 Urol*. 2018;15(10):615-25. 780

- 775 [6] Malmstrom PU, Sylvester RJ, Crawford DE, Friedrich
776 M, Krege S, Rintala E, Solsona E, Di Stasi SM, Wit-
777 jes JA. An individual patient data meta-analysis of the
778 long-term outcome of randomised studies comparing intravesi-
779 cal mitomycin C versus bacillus Calmette-Guerin for
780 non-muscle-invasive bladder cancer. *Eur Urol.* 2009;56(2):
781 247-56.
- 782 [7] Sylvester RJ, van der Meijden AP, Oosterlinck W, Witjes
783 JA, Bouffouix C, Denis L, Newling DW, Kurth K. Predicting
784 recurrence and progression in individual patients with stage
785 Ta T1 bladder cancer using EORTC risk tables: a combined
786 analysis of 2596 patients from seven EORTC trials. *Eur*
787 *Urol.* 2006;49(3):466-5; discussion 75-7.
- 788 [8] Domingos-Pereira S, Cesson V, Chevalier MF, Derre
789 L, Jichlinski P, Nardelli-Haeffliger D. Preclinical efficacy
790 and safety of the Ty21a vaccine strain for intravesical
791 immunotherapy of non-muscle-invasive bladder cancer.
792 *Oncoimmunology.* 2017;6(1):e1265720.
- 793 [9] Domingos-Pereira S, Sathiyandan K, La Rosa S, Polak L,
794 Chevalier MF, Martel P, Hojeij R, Derre L, Haeffliger JA,
795 Jichlinski P, Nardelli-Haeffliger D. Intravesical Ty21a Vac-
796 cine Promotes Dendritic Cells and T Cell-Mediated Tumor
797 Regression in the MB49 Bladder Cancer Model. *Cancer*
798 *Immunol Res.* 2019;7(4):621-29.
- 799 [10] Samuel C, Reddington MH. Secrets of a covalent interaction
800 for biomaterials and biotechnology: SpyTag and Spy-
801 Catcher. *Current Opinion in Chemical Biology.* 2015(29):
802 94-99.
- 803 [11] van den Berg van Saparoea HB, Houben D, de Jonge MI,
804 Jong WSP, Luirink J. Display of recombinant proteins on
805 bacterial outer membrane vesicles by using protein ligation.
806 *Appl Environ Microbiol.* 2018;84:e02567-17.
- 807 [12] Zakeri B, Fierier JO, Celik E, Chittock EC, Schwarz-Linek
808 U, Moy VT, Howarth M. Peptide tag forming a rapid covalent
809 bond to a protein, through engineering a bacterial
810 adhesin. *Proc Natl Acad Sci U S A.* 2012;109(12):E690-7.
- 811 [13] Kavoussi LR, Brown EJ, Ritchey JK, Ratliff TL.
812 Fibronectin-mediated Calmette-Guerin bacillus attachment
813 to murine bladder mucosa. Requirement for the expression
814 of an antitumor response. *J Clin Invest.* 1990;1:62-67.
- 815 [14] Iwahi T, Abe Y, Nakao M, Imada A, Tsuchiya K. Role of
816 Type 1 fimbriae in the pathogenesis of ascending urinary
817 tract infection induced by *Escherichia coli* in mice. *Infect*
818 *Immun.* 1983;39(3):1307-15.
- 819 [15] Keith BR, Maurer L, Spears A, Orndorff PE. Receptor-
820 Binding Function of Type 1 Pili Effects Bladder
821 Colonization by a Clinical Isolate of *Escherichia coli*. *Infect*
822 *Immun.* 1986;53(3):693-96.
- 823 [16] Langermann S, Palaszynski SR, Barnhart M, Auguste G,
824 Pinkner JS, Burlein J, Barren P, Koenig S, Leath S, Jones
825 CH, Hultgren SJ. Prevention of mucosal *Escherichia coli*
826 infection by FimH-adhesin-based systemic vaccination.
827 *Science.* 1997;276(5312):607-11.
- 828 [17] Connell H, Agace W, Klemm P, Schembri M, Mar-
829 ilds S, Svanborg C. Type 1 fimbrial expression enhances
830 *Escherichia coli* virulence for the urinary tract. *Proc Natl*
831 *Acad Sci U S A.* 1996;93:9827-32.
- [18] Scheepbouwer C, Meyer S, Burggraaf MJ, Jose J, Molthoff
832 CF. A Multimodal Imaging Approach for Longitudinal
833 Evaluation of Bladder Tumor Development in an Orthotopic
834 Murine Model. *PLoS One.* 2016;11(8):e0161284.
835
- [19] Jonathon T Hill BLD, Brent W Bisgrove, Yi-Chu Su, Megan
836 Smith, H Joseph Yost. Poly Peak Parser: Method and Soft-
837 ware for Identification of Unknown Indels Using Sanger
838 Sequencing of Polymerase Chain Reaction Products. *Develop-*
839 *mental Dynamics.* 2014;243(12):1632-36.
840
- [20] Li L, Fierier JO, Rapoport TA, Howarth M. Structural anal-
841 ysis and optimization of the covalent association between
842 SpyCatcher and a peptide Tag. *J Mol Biol.* 2014;426(2):
843 309-17.
844
- [21] Jong WSP, Daleke-Schermerhorn MH, Vikström D, ten
845 Hagen-Jongman CM, de Punder K, van der Wel N, van
846 de Sandt CE, Rimmelzwaan GF, Follmann F, Agger E,
847 Andersen P, de Gier J, Luirink J. An autotransporter display
848 platform for the development of multivalent recombinant
849 bacterial vector vaccines. *Microb Cell Fact.* 2014;13(162).
850
- [22] Luo Y, Chen X, Han R, Chorev M, Dewolf WC, O'Donnell
851 MA. Mutated RAS p21 as a target for cancer therapy in
852 mouse transitional cell carcinoma. *J Urol.* 1999;162(4):
853 1519-26.
854
- [23] Li R, Sundi D, Zhang J, Kim Y, Sylvester RJ, Spiess PE,
855 Poch MA, Sexton WJ, Black PC, McKiernan JM, Stein-
856 berg GD, Kamat AM, Gilbert SM. Systematic Review of the
857 Therapeutic Efficacy of Bladder-preserving Treatments for
858 Non-muscle-invasive Bladder Cancer Following Intravesical
859 Bacillus Calmette-Guerin. *Eur Urol.* 2020(78):387-99.
860
- [24] Brausi M, Oddens J, Sylvester R, Bono A, van de Beek C,
861 van Andel G, Gontero P, Turkeri L, Marreaud S, Collette
862 S, Oosterlinck W. Side effects of Bacillus Calmette-Guerin
863 (BCG) in the treatment of intermediate- and high-risk Ta,
864 T1 papillary carcinoma of the bladder: results of the EORTC
865 genito-urinary cancers group randomised phase 3 study
866 comparing one-third dose with full dose and 1 year with
867 3 years of maintenance BCG. *Eur Urol.* 2014;65(1):69-76.
868
- [25] Lamm DL, Blumenstein BA, Crissman JD, Montie JE,
869 Gottesman JE, Lowe BA, Sarosdy MF, Bohl RD, Gross-
870 man HB, Beck TM, Leimert JT, Crawford ED. Maintenance
871 Bacillus Calmette Guerin Immunotherapy for Recurrent TA,
872 T1 and Carcinoma in situ Transitional Cell Carcinoma of the
873 Bladder: A Randomized Southwest Oncology Group Study.
874 *J Urol.* 2000;163:1124-29.
875
- [26] Shlomi Tapiero AH, Daniel Kedar, Ofer Yossepowitch,
876 Andrei Nadu, Jack Baniel, David Lifshitz, David Margel.
877 Patient Compliance With Maintenance Intravesical Ther-
878 apy for Nonmuscle Invasive Bladder Cancer. *Urology.*
879 2018(118):107-13.
880
- [27] Fiorentino M, Lammers KM, Levine MM, Szein MB,
881 Fasano A. In vitro Intestinal Mucosal Epithelial Responses
882 to Wild-Type Salmonella Typhi and Attenuated Typhoid
883 Vaccines. *Front Immunol.* 2013;4:17.
884
- [28] Mulvey MA, Lopez-Boado YS, Wilson CL, Roth R, Parks
885 WC, Heuser J, Hultgren SJ. Induction and evasion of host
886 defenses by Type 1-piliated uropathogenic *Escherichia coli*.
887 *Science.* 1998;282:1494-97.
888